Physico-chemical characterization of playground sand dust, inhalable and bioaccessible fractions

(Article begins on next page)

15 December 2021

This is the author's final version of the contribution published as:

Iris H.Valido, Elio Padoan, Teresa Moreno, Xavier Querol, Oriol Font, Fulvio Amato

8
9

The publisher's version is available at:

When citing, please refer to the published version.

Chemico-physical characterization of playground sand dust, inhalable and bioaccessible fractions

Iris H.Valido [a,*], Elio Padoan[a-b], Teresa Moreno[a], Xavier Querol[a], Oriol Font[a], Fulvio Amato[a]

[a] Institute of Environmental Assessment and Water Research (IDÆA), Spanish National Research Council (CSIC), Barcelona, Spain

[b] Dipartimento di Scienze Agrarie, Forestali e Alimentari (DISAFA), Università degli Studi di Torino, Grugliasco (Torino), Italy

[*]Present address: Centre Grup de Tècniques de Separació en Química (GTS), Departament de Química, Universitat Autònoma de Barcelona, Bellaterra, Spain

Corresponding author:

Iris H. Valido

Centre Grup de Tècniques de Separació en Química (GTS), Departament de Química, Universitat Autònoma de Barcelona, Edifici C, Av. De l'Eix Central, s/n, 08193 Cerdanyola del Vallès, Barcelona, Spain.

iris.henriquez@uab.cat

Abstract

Dust is a mixture of natural and anthropogenic particles originated from multiple sources, which can represent an hazard for human health. Playgrounds are a site of particularly concern, due to sand dust ingestion by toddlers and inhalation. In this study, 37 sands used in public playgrounds in the city of Barcelona were physico-chemically characterized also in relation to routine maintenance activities such as disinfection and sand renewal. The analyzed sands show a felsic mineralogy dominated by Na-feldspar, quartz, and, to a lesser extent, K-feldspar, with minor amounts of clay minerals, carbonates and hematite. Particle fractions below 10, 2.5 and 1 µm represent, on average, 0.65%, 0.17% and 0.07% of bulk volume, respectively, although, due to the human grinding, these initial fractions increased every year by a 18%, 5% and 2% respectively. Disinfection of sands effectively reduced only the NH_4^+ concentration, among inorganic species. The average metal content was anthropogenically enriched, with respect to the upper continental crust, only for Sb and As. Both elements show high spatial variation indicating local sources such as road traffic for Sb (contributing mostly to the total concentration), and industry for As (also contributing with highly bioaccessible Sb, Cu and Zn). A clear inverse relationship between total concentrations of some elements and their leachable (Sb) and bioaccessible (Sb and Cr) fractions is observed. The most bioaccessible elements were Ca>Ni>Cu>Sr>Cd>Pb, all above the 25% of the total concentration. Bioaccessibility was higher for the carbonate-bearing particles and for the anthropic emitted metals (>50% of Ba, Cu, K, Pb and Zn).

1. Introduction

Dust is a mixture of natural and anthropogenic particles originated from multiple sources, which can represent a hazardous pollutant for human health via inhalation, ingestion, and, to a lesser extent, dermal contact (Paustenbach, 2000). A particularly sensible population is children, due to their higher inhalation rate and to the unintentional or deliberate ingestion of significant quantities of dust through hand-to-mouth contact (Ruby and Lowney, 2012; Acosta et al., 2009; Ljung et al., 2007; Banerjee, 2003; Calabrese et al., 1997). Incidental ingestion provides the primary pathway for human exposure; Shi et al. (2011) calculated that ingestion contributed 97.5% and 81.7% to the total exposure doses of non-carcinogenic and carcinogenic elements for children, and 91.7% and 52.9% for adults. The average amount of soil/sand dust ingested by a children has been calculated in various studies between 39 and 271 mg day^{-1}, with a central estimate of 100 mg day^{-1}, representing the average dust intake for children within 1-6 years (USEPA, 2011). In addition, particle inhalation has been found to cause increased risk for respiratory and cardio-vascular disease and to affect the neurodevelopment of children (Sunyer et al., 2015). In urban environment, children exposure to dust occurs mostly during playground activities, as most of playgrounds are unpaved and sand particles are continuously ground by playing activities.

Particle size distribution is relevant for inhalation and ingestion processes. Inhalation involves mostly particles below hundreds of microns, although 10 microns (thoracic fraction) is the most common cut-off size for defining hazardous atmospheric particulate matter (PM). Incidental ingestion requires soil particles that can adhere to human hands, being finer particles (generally <63 μm in diameter) the more efficient in this behavior (Choate et al., 2006; Ruby and Lowney, 2012; Yamamoto et al., 2006).

As stated by the last report of air quality in Europe (EEA, 2015), PM limit values are often exceeded in Europe, mostly due to road traffic, industrial and biomass burning emissions. In addition, power generation, soil dust and shipping are also significant sources of PM. In the Barcelona Metropolitan Area the PM10 daily limit value was exceeded until 2013, due to the high concentrations observed at specific sites such as the Sants (in 2012) and El Prat de Llobregat (in 2013) monitoring sites. In both stations, the exceedances were mainly due to the high concentrations of the mineral component of PM, namely mineral dust, which consists of primary particles, generally coarser than 1 μm, and composed mainly by Al, Si, Ca, Fe, K and Ti, among other typical crustal species. Mineral dust can be emitted by multiple sources, including local soil resuspension, African dust outbreaks, construction works, and traffic-induced resuspension. Soil resuspension can increase considerably PM$_{10}$ levels also in school environment with sandy playgrounds (Amato et al., 2014).

Concerning the ingestion pathway, only a part of the ingested particles can be adsorbed and reach the systemic circulation (i.e. the bioavailable fraction), and the oral bioaccessibility is defined as the fraction that

is soluble in the gastrointestinal environment and available for absorption (Ruby et al., 1999). Therefore, *in vitro* tests of bioaccessibility are useful tools to predict the relative bioavailability, improving the accuracy of risk assessments in a cost-effective manner. In last years, bioaccessibility tests for soils have been developed and validated through comparison to the results of *in vivo* tests for specific metals (Oomen et al., 2002; Zia et al., 2011).

In this study we investigated the physico-chemical properties of sand dust in 37 public playgrounds in the city of Barcelona in relation to the risk for inhalation and ingestion for children, with the aim of: i) understanding the impact of sand use (two years period) on particle size distribution and metal contents; ii) understanding the impact of the regular maintenance activities (sand replacement and disinfection); iii) quantify the oral bioaccessibility of metals and their main sources.

2. Methodology

2.1. Sampling and analytical treatment

Thirty-seven parks within the city of Barcelona (NE, Spain) were selected and sampled on 11-12 December 2014 based on (see Table SM1, in Supplementary Material) the:

- Time past from the last sand replacement (samples labelled as 01R to 12R). Replacement is performed with a 2-years frequency by the City Council. This selection allowed evaluating the impact of sand aging/grinding from December 2012 to October 2014. In order to minimize possible confounders due to disinfection and spatial variability, the selected playgrounds of this first batch were disinfected nearly at the same time and were located within the same district.

- Time past from the last disinfection (consisting in a cleaning of the top 10 cm layer with water at 90ºC) (samples labelled as 01D to 08D). Disinfection is performed with 2-months frequency by the City Council. The selected playgrounds were disinfected from 6th October to 29th November 2014 and, in order to minimize possible confounders due to renewal and spatial variability, the selected parks of this second batch had similar time past from the last renewal and were located as close as possible. Spatial distribution of metals in playgrounds in the area of Barcelona (includes samples labelled as 01E to 13E and 01C to 05 C). The selected playgrounds sands of this batch were all replaced on February 2014, except for 01, 03, 04 and 05C, and were spread across the city.

- Location: Playgrounds located across the municipal terrain, with sand replaced at the same time (February 2014). Samples labelled as 01E to 13E.
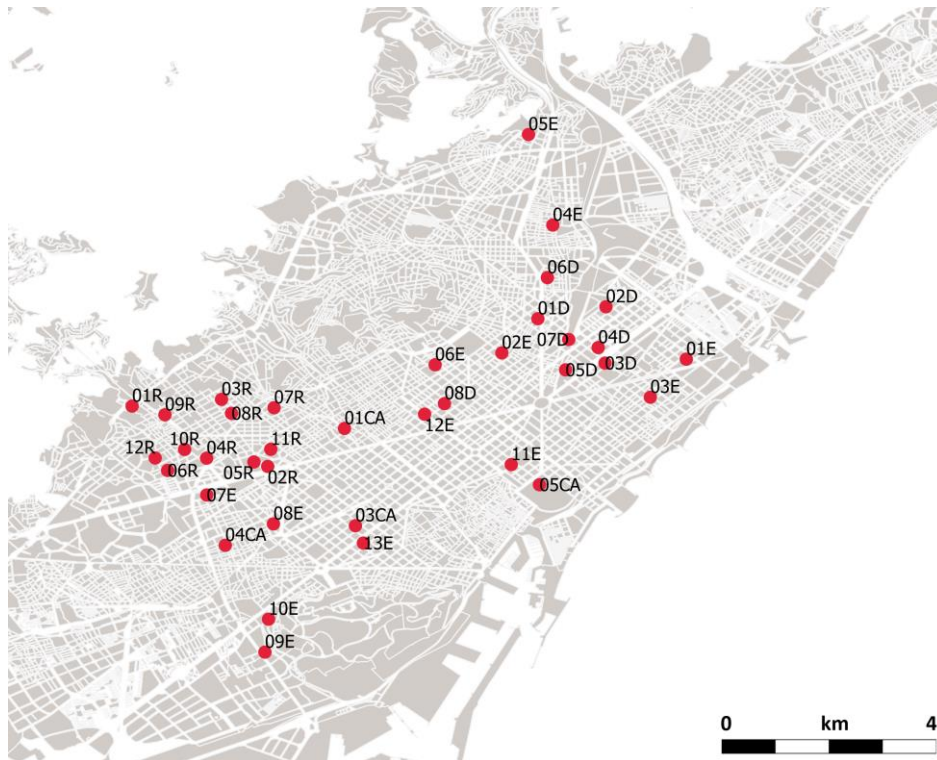
4

Figure 1. Map of playgrounds sampled across the city of Barcelona.

The sand sampling was performed within the top layer at 37 playgrounds using a PVC ring (5 cm height and 10 cm diameter), at two points of the playground (USEPA, 1992) not covered by the treetops, not at the edge of the playground or near to vegetation or urban furniture and visibly dry. Each of the two subsamples allowed the collection of 393 cm^3 of sand. In addition, one unexposed sand sample, not previously used for other purposes (blank), was collected from the stock of the provider in charge of the sand replacement. Once collected in a plastic bottle, samples were brought to the laboratory. Collected subsamples were mixed, homogenized and quartered to the final mass needed for laboratory analysis (Fernández, 2006; VMGA, 2014). Sand humidity and porosity were calculated gravimetrically, after drying the samples during 24h in a heater at 60ºC and adding Milli-Q water until saturation (Asensio et al., 2012). For each sample, 200 g of sand were then dried in plastic Petrie dishes in the stove at 60ºC during 24h, and sieved at 63 µm by means of a mechanic siever during 15 minutes.

Once sieved the (<63 µm) sample was divided into several fractions for different laboratory analyses:

- 5 g were leached in Milli-Q water for the determination of water soluble ions. To determine the leaching potential of major and trace elements, we applied the European Standard leaching test EN-12457 (according to Council decision 2003/33/EC), using a ratio liquid/solid (Milli Q water/sample) of 10:1 under shaking for 24h. Then, the leachate was filtered using a syringe (BRAUN Injekt 10ml) and a 0.45µm PVDF Whatman filter and the liquid part was analyzed: selective electrode for NH_4^+, High Performance Liquid Chromatography (HPLC Waters 1525) (for Cl^-, NO_3^-, and SO_4^{2-}), Inductively Coupled Plasma- Mass Spectrometry (ICP-MS, Thermo Fischer Scientific X-Series II), for trace elements) and Atomic Emission Spectrometry (ICP-AES, Thermo Fischer Scientific iCAP 6500

Radial) for major elements. The samples sent to both ICPs were acidified to 2% HNO_3. Besides that, the pH and ionic conductivity were determined by means of Thermo Scientific pHmeter and Ultrameter MyronL respectively.

- 150 mg were used for the grain size analysis, by means of a Malvern Mastersizer 2000 with Hydro 2000G. The sample was dispersed in Milli Q water and analyzed between 0.01 and 2000 µm. From the spectrometric pattern acquired, the particle size distribution is calculated using the model of Mie's scattering theory.

- 1.5 g of each sample were milled for: 1 g for X-Ray Diffraction (XRD), 0.1 g for acid digestion and 0.1 g to determine Total Carbon (TC) by means of an elemental LECO analyzer.

The powder XRD data were collected by a Bruker D8 A25 Advance X-ray diffractometer θ-θ, with $CuK_{\alpha 1}$ radiation, Bragg-Brentano geometry and a lineal LynxEyeXE detector. The XRD spectra were obtained from 4º to 60º of 2-Theta with a step pf 0.015º and a counting time of 0.1s and the sample rotation. The quantitative analyses on 9 samples were instead performed from 4º to 120º of 2-Theta with a step of 0.015º and a counting time of 0.5s and the sample in rotation. The crystalline phase identification was carried out by standard Joint Committee on Powder Diffraction Standards (JCPDS) file by the computer program "EVA" (Bruker).

For elemental composition, the samples (<63µm) were acid-digested adapting a protocol used for PM samples (Querol et al., 2001), using 5 ml HF, 2.5 ml HNO_3 and 2.5 ml $HClO_4$. For quality assurance, reference materials were also digested to determine the accuracy of the analytical and digestion methods: SRM 1633b (Trace Elements in Coal Fly Ash) and CANMET SO-2 and SO-4.

A widely used and tested method was used to assess the oral bioaccessibility: the Simple Bioaccessibility Extraction Method (SBET), consisting in an extraction with glycine at a buffered pH miming the conditions on the gastrointestinal tract of children (Drexler and Brattin, 2007; Oomen et al., 2002). Oral bioaccessible (SBET method) contents were determined mixing 0.25 g with 25 ml of extractant, a glycine 0.4 M solution with pH adjusted to 1.5 with concentrated HCl. Samples have been horizontally shaken at 37°C and 140 rpm for 1 h (Ruby et al., 1999; U.S. EPA, 2013). The mixture was then centrifuged at 3000 rpm for 10 min and the supernatant filtered through 0.45µm PVDF (Whatman) filters prior to analysis. The extract was analyzed for trace and major elements as above descript, except for P, S, As and V, not analyzed as the first two were present as impurities in the extracting solution and the last were highly interfered from the chloride.

2.3 Source apportionment of metals

Source apportionment techniques are used to apportion pollutants mass contributions to different source/factors which are able to explain most of the variance of observed pollutants concentrations. Source apportionment studies are generally performed by receptor models that are based on the mass conservation principle:

$$x_{ij} = \sum_{k=1}^{p} g_{ik} f_{jk} + e_{ij} \tag{1}$$

196

197 Where x_{ij} is the ith concentration of the species j, g_{ik} is the ith contribution of the source k and f_{jk} is the

198 concentration of the species j in source k , while e_{ij} are the residuals. Equation (1) can be also expressed in

199 matrix form as $\mathbf{X}=\mathbf{GF}^T$. If f_{jk} are known for all the sources then the Chemical Mass Balance (CMB) can be

200 applied (Watson et al., 1984). For this model the experimental profiles of all major sources are needed. When

201 both g_{ik} and f_{jk} are unknown, factor analysis (FA) techniques such as *Principal Components Analysis* (PCA)

202 (Henry and Hidy, 1979; Thurston and Spengler, 1985) and *Positive Matrix Factorization* (PMF) (Paatero and

203 Tapper, 1994) are used for solving (1).

204 PMF solves equation (1) minimizing the object function Q:

$$Q = \sum_{i=1}^{n} \sum_{j=1}^{m} (e_{ij} / s_{ij})^2 \tag{2}$$

205

206 where s_{ij} are the individual data uncertainties. For all elements with concentrations above the detection limit

207 the uncertainty was expressed as 10% of the element concentration plus one third of the detection limit. For

208 elements with concentration below or equal to the detection limit, uncertainty was expressed as 0.83 times

209 the detection limit. The PMF was applied using US EPA's PMF software, Version 5.0 (Norris et al., 2014).

210 A total (dependent) variable was set as a constant value (10^6 mg/kg) for all samples. The input data matrix

211 contained the 33 most significant elements/components concentrations, based on their signal-to-noise ratio

212 (Paatero and Hopke, 2003), the percentage of data above the detection limit and importance in tracing

213 specific sources. The distribution of residuals, G-space plots, Fpeak values and Q values were explored for

214 solutions with number of factors varying between 3 and 7.

215 The PMF method was also applied to the bioaccessible fraction of metals (µg/g) as independent variables,

216 setting the sum of analyzed species as total variable. The input data contained the 18 most significant

217 analyzed elements (excluding ions, As, P, S and V due to the extraction matrix and Ce, La, Li, Mo, Rb, Se,

218 Sn, Ti and Zr, with high percentage of values below detection limit).

219

220 **3. Results**

221

222 *3.1 Physico-chemical characteristics*

223 The chemical characterization of sand samples (fraction below 63 µm) of playgrounds in the city of

224 Barcelona is reported in Table 1, and shows a main aluminum-silicate composition (Al_2O_3 represents within

225 5.2-17.9 % of mass) followed by Ca-Mg carbonates (CaO+MgO sums within 0.5-10.1 % of mass).

226 Significant fractions of mass consist also of total carbon (TC), Fe_2O_3, K_2O, Na_2O and P_2O_5 (1.1±0.9%,

227 4.0±0.9%, 5.2±1.1%, 4.0±1.0%, 0.21±0.15%, respectively). The sum of SO_4^{2-}, NO_3^-, NH_4^+ and Cl^- represents

228 only 0.003-0.3% of the mass, while trace elements sum 0.2-1.0% of the mass. The most abundant trace

229　elements are Ti, Mn, Ba, Zr, Zn, Rb, and Sr, with mean concentrations of 3130, 894, 562, 369, 166, 158, and

230　80 µg/g, respectively.

231

232　Table 1. Total concentrations (µg/g), bioaccessible fraction (%) and leachable fraction (%) of the

233　analyzed metals. na: not analyzed

Element	Mean Total concentration (µg/g)	Mean bioaccessible fraction (%)	Mean leachable fraction (%)	Element	Mean Total concentration (µg/g)	Mean bioaccessible fraction (%)	Mean leachable fraction (%)
Al	75571	1	<0.1	Ni	9.3	44	<0.1
As	12	na	0.2	P	0.05	na	1
Ba	561	8	<0.1	Pb	62	27	<0.1
Ca	15954	64	2	Rb	158	<1	<0.1
Cd	0.97	30	0.2	S	93	na	7
Co	3.7	21	0.1	Sb	2.2	14	3
Cr	19	20	<0.1	Se	1.1	41	0.3
Cu	26	36	0.2	Sn	18	< 0.1	<0.1
Fe	27852	1	<0.1	Sr	81	28	1
K	37670	1	<0.1	Ti	3147	0.5	<0.1
La	57	8	<0.1	U	10	4	<0.1
Li	27	2	0.4	V	40	na	<0.1
Mg	4496	17	0.6	W	14	22	2
Mn	887	24	0.1	Zn	166	16	<0.1
Mo	1.4	4	6	Zr	361	<0.1	<0.1
Na	26846	1	<0.1				

234

235　We calculated the Enrichment Factors (EFs) for all elements, normalizing the concentration of the element

236　with the concentration of Al in the average Earth upper-crust (Taylor and McLennan, 1995). Mean values for

237　samples are reported in Figure SM1, in the Supplementary Material, together with values for the unexposed

238　sand sample (blank). The majority of the elements appear not to be significantly enriched in sands, averaging

239　all samples, while only As, Cd and Sb showed EFs around 10 (9, 10 and 12, respectively). With respect to

240　the unexposed sample, however, only As and Sb showed enrichment, which is noteworthy considering the

241　little time of exposure of sand to the atmospheric metals deposition.

242　The sand particle grain size (% in volume) shows a typically coarse size distribution (Figure SM2) being the

243　inhalable fraction (below 63 µm) 3.72% on average. The presence of clay minerals and mica is likely

244　responsible for the significant fraction of particles below 2 µm. The thoracic fraction (<10 µm) accounted

245　typically for 0.65% of bulk volume (or mass, assuming constant particle density), while the fraction below

246　2.5 and 1 µm are in average 0.17% and 0.07%, respectively.

247　*3.2 Mineralogy*

248 The XRD results (Table SM2) show a felsic mineralogy dominated by Na-feldspar, quartz, and, to a lesser

249 extent, K-feldspar, with minor amounts of clay minerals (illite>chlorite), carbonates (mostly calcite) and

250 traces of hematite.

251 According to the quantitative estimate of relative amounts on 9 samples (batch D: samples with same time of

252 use and the unexposed sample), Na-feldspar is the most common mineral present (27-48%), followed by K-

253 feldspar (13-23%) and quartz (9-23%). Illite and chlorite amounts range within 11-27% and 6-11%

254 respectively. In addition, dolomite and calcite were also detected although not in all the samples and up to

255 6% and 4% of total mass, while hematite was only in trace content.

256 The source for these feldspathic sandstones is likely to be mainly from weathered granites (possibly with

257 some influence from metamorphic materials). Much of the illite could derive from altered muscovite mica,

258 the chlorite and hematite from altered biotite mica, and the calcite from the minor amount of calcium present

259 in Na-feldspar.

260 With regard to the geology surrounding Barcelona, there is more exposure of the Palaeozoic granitoid

261 basement around the River Besos valley than the Llobregat (although there is granodiorite exposed at least as

262 far SW as the hill of Sant Pere Martir, and this may have fed granitic material into the Llobregat at least

263 since Plio-Pleistocene times). The thick Pleistocene sediments flanking the Collserola hills generally contain

264 much weathered granitic detritus. The abundance of feldspar makes these sandstones sedimentologically

265 immature, so it is likely that they are sourced from mostly local materials deposited fluvially.

266 The mineralogy affects particle size distribution as when the percentage of quartz increases, the fraction (in

267 volume) of soil particles below 10 microns decreases ($R^2= 0.56$), due to the coarser size distribution of quartz

268 particles (the same was expected for the fractions below 2.5 and 1 microns, but the trendwas not so clear).

269 The potential impact on emissions due to resuspension is therefore lower for quartz-rich sands, rather than

270 for typical fluvial sands, enriched in feldspars and fine clay minerals.

271

272 *3.3 Effects of maintenance activities*

273 One of the main goals of the study was to evaluate the impact of sand use (i.e. time past from the last sand

274 replacement) on the physico-chemical characteristics. Regarding the particle size distribution, it can be

275 observed a general increasing proportion of respirable fractions with the time of use (Figure SM3). Sands

276 become therefore finer over time, by an average rate of 17.7%, 4.7% and 2.0%, for the fractions <10 μm,

277 <2.5 μm and <1 μm respectively, per year.

278 Figure 2 shows the full size distribution of particle volume for three samples collected after 6, 14 and 21

279 months of use, respectively. It can be clearly observed the increase in fraction below 20 μm (from the

280 "youngest" (less used sand: 20%) to the "oldest" sample (more used sand: 49%)) in terms of their use in

281 public playgrounds.

282
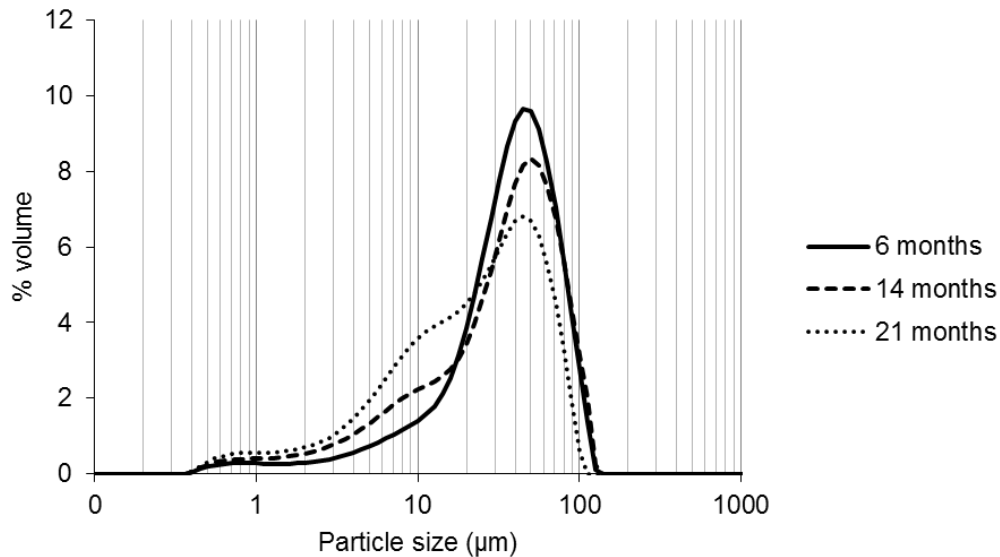
Figure 2. Size distribution of particle volume in sand samples collected after 6, 14 and 21 months of use.

Concerning the metal content, results show no clear impact of time of use on the buildup of metals, probably due to the relatively little time of exposure (<2 years). Unexpectedly, some metals such as Cr, Ni and Pb show higher concentrations in sands newly replaced, suggesting a relevant contribution from bedrock materials such as carbonates (Cr and Ni, see section 3.5) and feldspars (Pb, see section 3.5). Similarly, neither TC nor soluble compounds showed higher concentrations in the "oldest" samples.

Regarding the treatment of disinfection that is carried out every 2 months in the playgrounds, it can be observed that the effect on the inorganic fraction of sand is limited to a decreasing trend on the concentration of NH_4^+ (Figure SM4). The NH_4^+ concentration seems to increase exponentially with time after the last disinfection (R^2=0.58), probably due to the atmospheric deposition of ammonium salts. No clear effect on other soluble components, such as SO_4^{2-}, NO_3^- or Cl^- was found. Neither metals seem to have been affected by this treatment, due to their low solubility in water (<6%). No effect on particle size distribution was found.

3.4 Spatial variability

Enrichment factors were explored in the spatial domain of the city. Cadmium, as shown earlier, was enriched by a factor of 9 with respect to the Earth crust, but not enriched with respect to the local unexposed sand. The range of enrichment variability was low across the city (Figure 3), showing a maximum EF of 1.6 (with respect to the unexposed sand). Conversely As showed a clearer spatial pattern in the anthropogenic signature across the city, displaying maxima enrichments towards the coastal part of the city, although no clear association to specific sources can be drawn. Antimony, manly emitted from non-exhaust sources (Schauer et al., 2006), showed also little variation across the city, however no correlation was found between metals concentrations and time of exposure or traffic density.
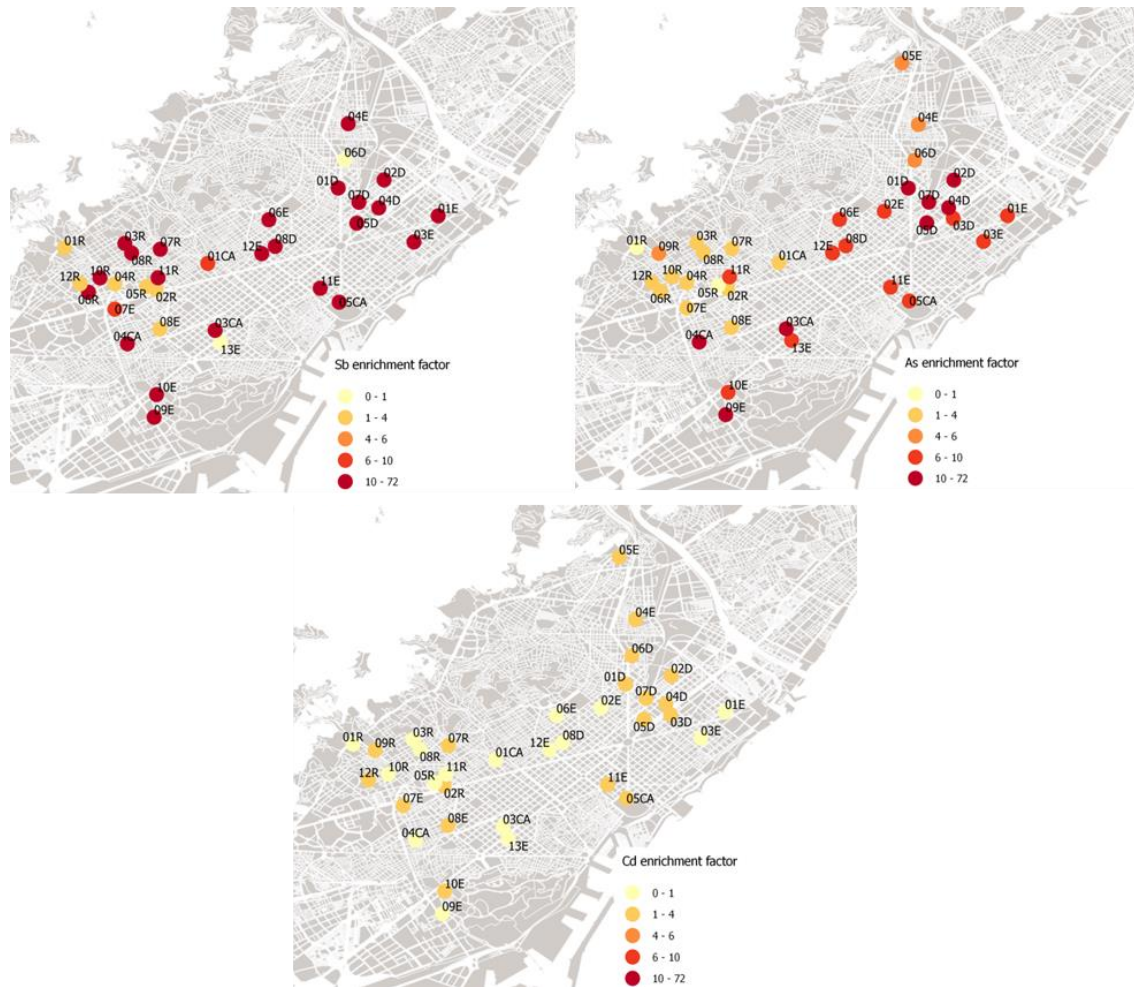
10

Figure 3. Maps of Enrichment factors calculated for Sb, As and Cd with respect to the unexposed sand.

Spatial Distribution analysis revealed also higher levels of NO_3^- and NH_4^+ in parks located in the NE part of the city (Figure SM5), next to a methane-fueled power plant, although this part of the city, which is at the lowest altitude and a shallow top layer of the phreatic zone, can be also influenced by leaking from sewage system.

3.5 Source apportionment of metals

The PMF solution for total metal concentrations (<63 µm) revealed four factors/sources, namely Anthropogenic, Al-Silicates, Salts and Carbonates (Figure 4). These sources contributed, in average, 4.3%, 57.6%, 10.6% and 27.5% to the sand material below 63 µm.
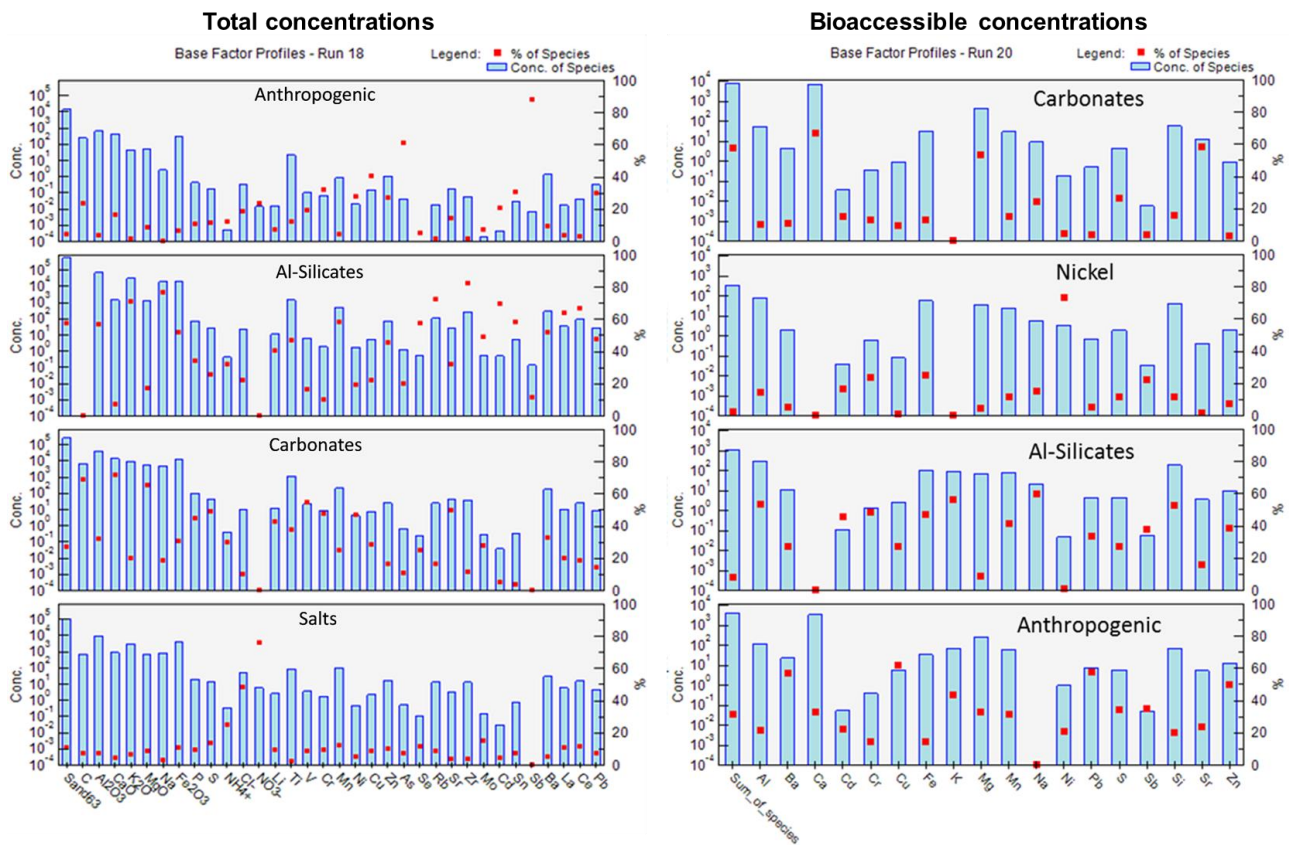
Figure 4. PMF factor profiles for total (left) and bioaccessible (right) concentrations. Blue bars indicate average absolute species concentration (mg/kg, left axis), red dots indicate % of specie due to each source.

The Anthropogenic source was identified from the high share of Sb, As, Cu explained by this source. Sb and Cu are commonly used as brake wear tracers (Schauer et al., 2006), but can also be emitted by metallurgical industry (Amato et al., 2009), as for As. The chemical profile of this factor is dominated by Fe_2O_3, C, S, Al_2O_3 and CaO. It is also noteworthy the significant share of Sn, Cr, Pb and Mn explained by this source.

The Al-Silicates source is the main responsible for the total composition, explaining most of the variation of Al_2O_3, NaO, K_2O, Fe_2O_3, Rb, Ti and Mn, which are related to clay minerals (illite, and chlorite) and feldspars (microcline and albite). This factor also shows the majority of Zr, Sn and Pb, which all have affinity to aluminum silicates.

The third factor, labelled as Salts, explained most of Cl^- and NO_3^- variation, and (to a lesser extent) NH_4^+, suggesting the presence of ammonium salts and sea salt from atmospheric deposition.

The fourth factor is clearly related to carbonates, showing high loading of CaO, MgO, C, but also Sr, Ba and Ni, which are quite common in calcite and dolomite. The presence of S and Ba may indicate also the presence of barite.

According to PMF results, more than 50% of S, Cu, Sb, and As in sands are originated from anthropogenic sources, although only As and Sb show high enrichment factors with respect to the average composition of Earth crust and the unexposed sand.

340 In spite of the clear anthropogenic contribution (related, probably, mainly to traffic and industry), no
341 correlation was found between the anthropogenic factor and the traffic density (vehicles m^{-2}, data provided
342 from the Catalan Government, Table SM1), suggesting that the most relevant traffic contribution is from
343 background rather than from street-level emissions.
344

345 *3.6 Leachable and bioaccessible fractions*
346 The pH of the leachates of the playground sands are slightly alkaline, with values ranging from 7.1 to 7.9.
347 Mean leachable fraction of each element is listed in Table 1. The most soluble elements were S, Mo, Sb, Ca,
348 and Sr, although their soluble fraction does not exceed 7%, 6%, 3%, 2% and 1%, respectively. Therefore, the
349 solubility is not related to specific sources, as S and Mo are mostly explained from the Al-Silicates factor, Sb
350 from the Antrrhropogenic and Ca and Sr from the Carbonates factor.
351 In several elements (i.e. Sb, Ca, Cd Zn, Cr, Zr, Ni, Sr and Mg) it has been observed that the higher the total
352 concentration of the element (μg/g), the lower the leachable fraction (%), which might suggest a different
353 speciation and solubility of the metals emitted by the different sources. Antimony, for example, (see Figure
354 SM6, in Supplementary Material) was found to be mostly anthropogenic (as shown by PMF results),
355 showing a higher solubility at lower concentrations, especially in the SW part of the city, which suggests a
356 more industrial (with high temperature process and finer size distribution) origin of the bioaccessible
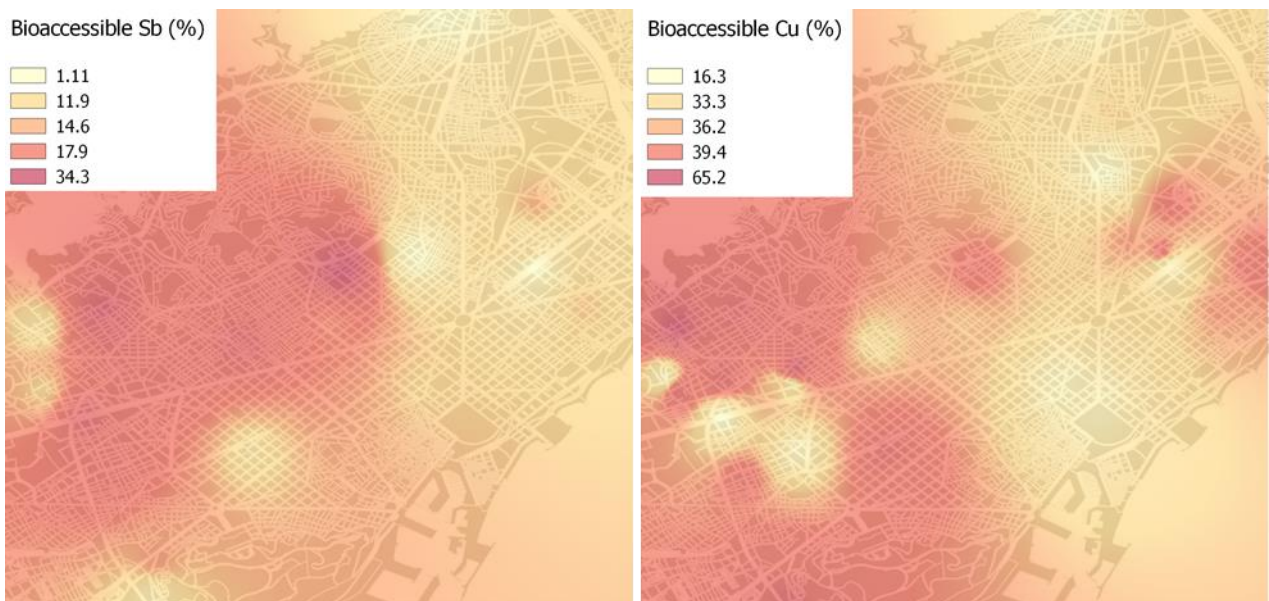357 fraction.
358 Bioaccessibility extraction test is used to determine the metal fraction that would dissolve in the gastric
359 environment and become available for absorption. Results for all analyzed elements are reported in Table 1
360 as percentage of the total content.
361 Average values of bioaccessibility varies from 0.002% of Zr to 64% of Ca , but some of the most harmful
362 metals, such as Ni, Cu, Cd, Pb and Sb, were also among the most bioaccessible (from 14% to 41%),
363 including Se.
364 The leachable fraction of Sb and Cr showed lower bioaccessible percentages in samples with higher
365 concentrations (Figure SM7). As for total concentration, the relationhip between the bioaccessible fraction
366 with disinfection and time of use was explored but no significant relationships were seen.
367 Spatial distribution of the bioaccessible contents was explored across the city. Cadmium, which showed the
368 higher variability range for bioaccessibility, did not show a clear spatial pattern, coherently with the
369 relatively low anthropogenic contribution. Antimony showed a higher bioaccessibility in the SW region of
370 the city (Figure 5), although this does not exceed 35%, where also the lowest concentrations were found.
371 Therefore road traffic, responsible for most (80%) of the Sb, produces probably less bioaccessible Sb than
372 industrial processes. This is in agreement with studies indicating that natural and mechanical wear
373 contribution is less bioaccessible than high temperature emission processes (Ljung et al., 2007; Madrid et al.,
374 2008; Wang et al., 2015). In fact, no relationship was found between traffic density and bioaccessible
375 relative (or absolute) concentrations of metals. Similarly to Sb, higher bioaccessibility in the SW of the city
376 was found for Cu and Zn, which are emitted from both traffic and industrial combustion sources (Amato et

377 al., 2009; Minguillón et al., 2012) but a higher bioaccessibility for the industrial emitted particles can be

378 deduced (Wang et al., 2015).

379

380

381 Figure 5. Spatial interpolation of the bioaccessible fraction (%) of Sb and Cu across the city of

382 Barcelona.

383

384 The PMF analysis applied to the bioaccessible metal concentrations (Figure 4) revealed four factors,

385 similarly to the solution found for the total metal concentration. The similar sources identified were

386 Carbonates, Anthropogenic and Al-Silicates, while and a Nickel factor (contributing very little to the sum of

387 species) was found instead of the Salts factor. Relative contribution to the sum of bioaccessible species was,

388 on average, 58%, 32%, 8% and 2%, respectively. Unfortunately, no separation of the Anthropogenic factor

389 could be achieved. These results are coherent with the first PMF if we consider that the Salts factor could not

390 be resolved, as in the SBET extract ions were not analyzed. Factor profiles are reported in Figure 4, while in

391 Figure 6 the contribution of each factor to the total concentration.

392
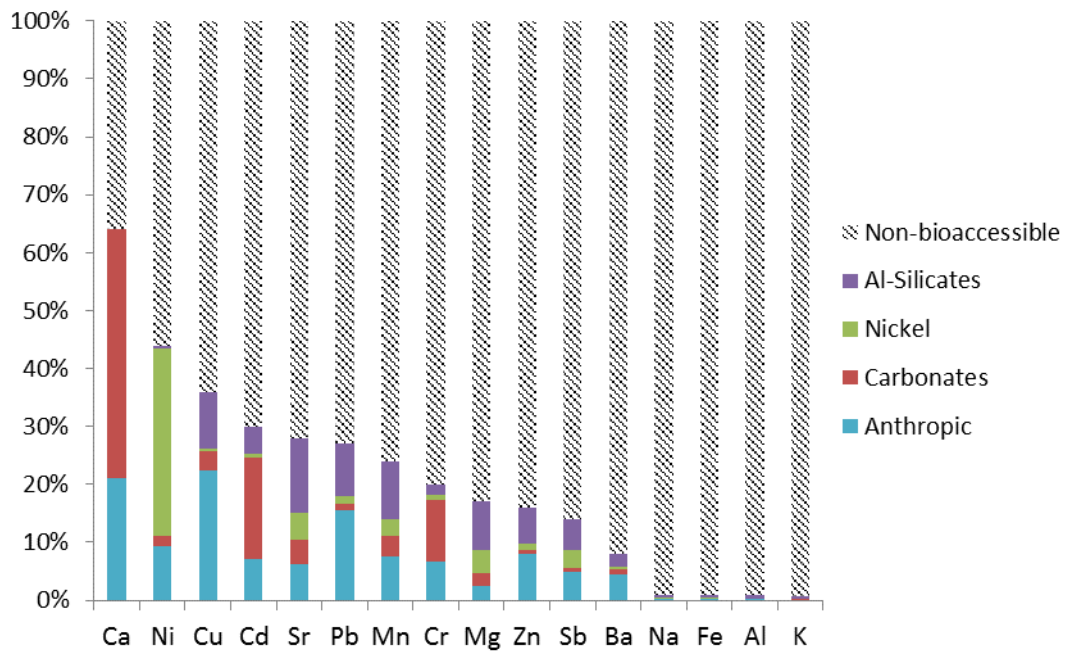
393

394 Figure 6. Share of bioaccessible metals explained from each factor, as fraction of the total

395 concentration.

396

397 According to PMF results, bioaccessible Sr, Mg, Cd and Ca are mainly explained by the Carbonates factors

398 and, as expected, are among the most available; as carbonates dissolve at gastric pH, while elements

399 explained mostly from the Al-Silicates factor are the least bioavailable, in average. More in detail, after Ca,

400 the most bioaccessible metal is Ni, associated mostly to the Nickel factor and to the Anthropogenic, and this

401 value is higher than what found in literature (Ljung et al., 2007; Padoan et al., 2016). Elements mainly

402 explained by the Anthropogenic factor, as Cu and Sb, have a bioaccessible fraction of 36% and 14%,

403 respectively, and also some Al-Silicates bearing metals, like Cd, Pb and Zn, have significant bioaccessible

404 fraction. The mass of the Anthropogenic factor is dominated by Ca, Mg and Al, and it explains most of the

405 variation of Ba, Cu, K, Pb and Zn.

406 Comparing PMF results for bioaccessible and total metal concentrations, the variation of metals explained by

407 the different factors is generally similar except for Ba and K, whose bioaccessible fraction derives more from

408 the Anthropogenic factor rather than geogenic (as for the total concentration), indicating that the anthropic

409 input for these metals is more bioaccessible than the natural one, which dominates the total concentration,

410 and Cr, shifting from the Carbonates to Al-silicates factor. Also Cu and Zn have a clearer anthropic signature

411 in the bioaccessible fraction, rather than the total concentration, which helps identifying spatial patterns (see

412 Figure 5 for Cu). The Ni-factor also shows significant contributions of Fe and Cr, pointing to steel particles.

413 However, the identification of this factor is not definitively clear.

414

4. Conclusions

Thirty-seven sands used in public playgrounds in the city of Barcelona were physico-chemically characterized in order to improve our understanding of their potential impact on risks due to dust ingestion by toddlers and inhalation. Routine maintenance activities were controlled, such as disinfection and sand replacement. The analyzed sands show a felsic mineralogy dominated by Na-feldspar, quartz, and, to a lesser extent, K-feldspar, with minor amounts of clay minerals (illite > chlorite), carbonates (mostly calcite) and traces of hematite. The particle size analysis shows a typically coarse distribution, although clay minerals are responsible for the significant fraction of particles below 2.5 µm. The fractions below 10, 2.5 and 1 µm represent, on average, 0.65%, 0.17% and 0.07% of the bulk volume, respectively, although due to the human grinding through playing, these initial fractions increase every year by a 18%, 5% and 2% respectively, confirming the environmental concern for air quality due to dust resuspension, which may cause local exceedances of PM_{10} European limit standards. Bimonthly disinfection of sands was found to reduce significantly only the NH_4^+ concentration. The average metal content was anthropogenically enriched with respect to the upper continental crust, only for Sb (EF=12) and As (EF=10), while the enrichment of Cd (EF=9) may be linked to the local geology. Both Sb and As show high spatial variation, attributed to the anthropogenic source in PMF, although no clear separation can be done between industrial and road traffic contributions. The spatial distribution suggests background road traffic and industry as main sources of Sb (as no correlation was found with street level traffic density) and, less clearly, harbor and industry as main sources of As. A clear inverse relationship between total concentrations of some elements and their leachable (Sb) or bioaccessible (mostly Sb and Cr) fractions is observed. The most bioaccessible elements were Ca>Ni>Cu>Sr>Cd>Pb, all above the 25% of the total concentration. Bioaccessibility was higher for the carbonate-bearing particles and for the anthropic emitted metals, being more than 50% of the bioaccessible fraction of Ba, Cu, K, Pb and Zn originated from the anthropogenic source.

Acknowledgements

Bibliography

Acosta, J.A., Cano, A.F., Arocena, J.M., Debela, F., Martínez-Martínez, S., 2009. Distribution of metals in soil particle size fractions and its implication to risk assessment of playgrounds in Murcia City (Spain). Geoderma 149, 101–109. Doi:10.1016/j.geoderma.2008.11.034.

Amato, F., Pandolfi, M., Escrig, A., Querol, X., Alastuey, A., Pey, J., Perez, N., Hopke, P.K., 2009. Quantifying road dust resuspension in urban environment by Multilinear Engine: A comparison with PMF2. Atmospheric Environment, 43 (17), pp. 2770-2780. Doi: 10.1016/j.atmosenv.2009.02.039.

450 Amato, F., Rivas, I., Viana, M., Moreno, T., Bouso, L., Reche, C., Àlvarez-Pedrerol, M., Alastuey, A.,
451   Sunyer, J., Querol, X., 2014. Sources of indoor and outdoor PM2.5 concentrations in primary
452   schools. Sci. Total Environ. 490, 757–765. Doi:10.1016/j.scitotenv.2014.05.051.

453 Asensio, I., Moreno, S., Blanquer, H.G., Manuel, J., 2012. Técnicas de medida del espacio poroso del suelo.
454   http://hdl.handle.net/10251/16872.

455 ASPB, Agencia de Salut Publica de Barcelona. Informe d'avaluació de la qualitat de l'aire a la ciutat de
456   Barcelona Any 2012, 2013. http://www.aspb.cat/quefem/docs/Qualitat_aire_2012.pdf.

457 Banerjee, A.D., 2003. Heavy metal levels and solid phase speciation in street dusts of Delhi, India. Environ.
458   Pollut. 123, 95–105. Doi: 10.1016/S0269-7491(02)00337-8.

459 Calabrese, E.J., Stanek, E.J., James, R.C., Roberts, S.M., 1997. Soil ingestion: A concern for acute toxicity in
460   children. Environ. Health Perspect. 105, 1354–1358.

461 Choate, L.M., Ranville, J.F., Bunge, A.L., Macalady, D.L., 2006. Dermally adhered soil: 1. Amount and
462   particle-size distribution. Integr. Environ. Assess. Manag. 2, 375–384. Doi:
463   10.1002/ieam.5630020409

464 Drexler, J.W., Brattin, W.J., 2007. An In Vitro Procedure for Estimation of Lead Relative Bioavailability:
465   With Validation. Hum. Ecol. Risk Assess. Int. J. 13, 383–401. Doi:10.1080/10807030701226350

466 EEA, 2015. Air quality in Europe — 2015 report. European Environment Agency, EEA Report No 5/2015.

467 Fernández, L. et al., 2006. Manual de técnicas de análisi de suelos aplicadas a la remediación de sitios
468   contaminados. Instituto Mexicano del Petróleo, Secretaría de Medio Ambiente y Recursos Naturales,
469   Instituto Nacional de Ecología, México.

470 Henry, R.C., Hidy, G.M., 1979. Multivariate analysis of particulate sulfate and other air quality variables by
471   principal components-Part I. Atmospheric Environ. 1967. Doi:10.1016/0004-6981(79)90068-4

472 Ljung, K., Oomen, A., Duits, M., Selinus, O., Berglund, M., 2007. Bioaccessibility of metals in urban
473   playground soils. J. Environ. Sci. Health Part A 42, 1241–1250. Doi:10.1080/10934520701435684

474 Madrid, F., Biasioli, M., Ajmone-Marsan, F., 2008. Availability and bioaccessibility of metals in fine
475   particles of some urban soils. Arch. Environ. Contam. Toxicol. 55, 21–32. Doi:10.1007/s00244-007-
476   9086-1

477 Minguillón, M.C., Schembari, A., Triguero-Mas, M., de Nazelle, A., Dadvand, P., Figueras, F., Salvado,
478   J.A., Grimalt, J.O., Nieuwenhuijsen, M., Querol, X., 2012. Source apportionment of indoor, outdoor
479   and personal PM2.5 exposure of pregnant women in Barcelona, Spain. Atmospheric Environ., 59,
480   pp. 426-436. Doi: 10.1016/j.atmosenv.2012.04.052

481 Norris, G., Duvall, R., Brown, S. and Bai, S., 2014. EPA Positive Matrix Factorization (PMF) 5.0
482   Fundamentals and User Guide, EPA/600/R-14/108. Environ. Prot. Agency Off. Researc Dev.
483   Publushing House Whashington DC 20460.

484 Oomen, A.G., Hack, A., Minekus, M., Zeijdner, E., Cornelis, C., Schoeters, G., Verstraete, W., Van de
485   Wiele, T., Wragg, J., Rompelberg, C.J.M., Sips, A.J.A.M., Van Wijnen, J.H., 2002. Comparison of

486   Five In Vitro Digestion Models To Study the Bioaccessibility of Soil Contaminants. Environ. Sci.
487   Technol. 36, 3326–3334. Doi:10.1021/es010204v

488   Paatero, P., Hopke, P.K., 2003. Discarding or downweighting high-noise variables in factor analytic models,
489   in: Analytica Chimica Acta. pp. 277–289. Doi:10.1016/S0003-2670(02)01643-4

490   Paatero, P., Tapper, U., 1994. Positive Matrix Factorization - A Nonnegative Factor Model with Optimal
491   Utilization of Error Estimates of Data Values. Environmetrics 5, 111–126.
492   Doi:10.1002/env.3170050203

493   Padoan, E., Romè, C., Ajmone Marsan, F., 2016. Bioaccessibility and size distribution of metals in road dust
494   and roadside soils along a peri-urban transect. Sci. Total Environ. 601-602, 89-98.
495   Doi:10.1016/j.scitotenv.2017.05.180

496   Paustenbach, D.J., 2000. The practice of exposure assessment: a state-of-the art review. J. Toxicol. Environ.
497   Health Part B 3, 179–291. Doi:10.1080/10937400050045264

498   Querol, X., Alastuey, A., Rodriguez, S., Plana, F., Mantilla, E., Ruiz, C.R., 2001. Monitoring of PM10 and
499   PM2.5 around primary particulate anthropogenic emission sources. Atmos. Environ. 35, 845–858.
500   Doi:10.1016/S1352-2310(00)00387-3

501   Ruby, M.V., Lowney, Y.W., 2012. Selective Soil Particle Adherence to Hands: Implications for
502   Understanding Oral Exposure to Soil Contaminants. Environ. Sci. Technol. 46, 12759–12771.
503   Doi:10.1021/es302473q

504   Ruby, M.V., Schoof, R., Brattin, W., Goldade, M., Post, G., Harnois, M., Mosby, D.E., Casteel, S.W., Berti,
505   W., Carpenter, M., Edwards, D., Cragin, D., Chappell, W., 1999. Advances in Evaluating the Oral
506   Bioavailability of Inorganics in Soil for Use in Human Health Risk Assessment. Environ. Sci.
507   Technol. 33, 3697–3705. Doi:10.1021/es990479z

508   Schauer, J.J., Lough, G.C., Shafer, M.M., Christensen, W.F., Arndt, M.F., DeMinter, J.T., Park, J.-S., 2006.
509   Characterization of metals emitted from motor vehicles. Res. Rep. Health Eff. Inst. 1-76-88.

510   Shi, G., Chen, Z., Bi, C., Wang, L., Teng, J., Li, Y., Xu, S., 2011. A comparative study of health risk of
511   potentially toxic metals in urban and suburban road dust in the most populated city of China. Atmos.
512   Environ. 45, 764–771. Doi:10.1016/j.atmosenv.2010.08.039

513   Sunyer, J., Esnaola, M., Alvarez-Pedrerol, M., Forns, J., Rivas, I., López-Vicente, M., Suades-González, E.,
514   Foraster, M., Garcia-Esteban, R., Basagaña, X., others, 2015. Association between traffic-related air
515   pollution in schools and cognitive development in primary school children: a prospective cohort
516   study. PLoS Med 12, e1001792. Doi: 10.1371/journal.pmed.1001792

517   Taylor, S.R., McLennan, S.M., 1995. The geochemical evolution of the continental crust. Rev. Geophys. 33,
518   241–265. Doi: 10.1029/95RG00262

519   Thurston, G.D., Spengler, J.D., 1985. A quantitative assessment of source contributions to inhalable
520   particulate matter pollution in metropolitan Boston. Atmospheric Environ. - Part Gen. Top. 19, 9–25.
521   Doi:10.1016/0004-6981(85)90132-5

522   U.S. EPA, 1992. Preparation of soil sampling protocols: Sampling techniques and strategies. U.S.
523   Environmental Protection Agency, EPA/600/R-92/128.
524   U.S. EPA, 2011. Exposure Factors Handbook 2011 Edition (Final). U.S. Environmental Protection Agency,
525   EPA/600/R-09/052F.
526   U.S. EPA, 2013. Method 1340, In vitro bioaccessibility assay for lead in soil. U.S. Environmental Protection
527   Agency, SW-846 Update VI.
528   VMGA, 2014. Vice Ministerio de Gestión Ambiental, D.G. de C.A., 2014. Guía para muestreo de suelos.
529   Wang, Q., Ma, Y., Tan, J., Zheng, N., Duan, J., Sun, Y., He, K., Zhang, Y., 2015. Characteristics of size-
530   fractionated atmospheric metals and water-soluble metals in two typical episodes in Beijing.
531   Atmospheric Environ., 119, 294-303. Doi:10.1016/j.atmosenv.2015.08.061
532   Watson, J.G., Cooper, J.A., Huntzicker, J.J., 1984. The effective variance weighting for least squares
533   calculations applied to the mass balance receptor model. Atmospheric Environ. - Part Gen. Top. 18,
534   1347–1355. Doi:10.1016/0004-6981(84)90043-X
535   Yamamoto, N., Takahashi, Y., Yoshinaga, J., Tanaka, A., Shibata, Y., 2006. Size distributions of soil
536   particles adhered to children's hands. Arch. Environ. Contam. Toxicol. 51, 157–163.
537   Doi:10.1007/s00244-005-7012-y
538   Yu, B., Wang, Y., Zhou, Q., 2014. Human Health Risk Assessment Based on Toxicity Characteristic
539   Leaching Procedure and Simple Bioaccessibility Extraction Test of Toxic Metals in Urban Street
540   Dust of Tianjin, China. PLoS ONE 9, e92459. Doi:10.1371/journal.pone.0092459
541   Zia, M.H., Codling, E.E., Scheckel, K.G., Chaney R.L., 2011. In Vitro and in Vivo Approaches for the
542   Measurement of Oral Bioavailability of Lead (Pb) in Contaminated Soils. Environmental Pollution
543   159, 2320-2327. Doi:10.1016/j.envpol.2011.04.043